International Journal of Pure and Applied Mathematics
Volume 101 No. 2 2015, 289-300
ISSN: 1311-8080 (printed version); ISSN: 1314-3395 (on-line version)
url: http://www.ijpam.eu
doi: http://dx.doi.org/10.12732/ijpam.v101i2.13

ijpam.eu

DYNAMICS AND CONTROL DESIGN VIA LQR AND SDRE METHODS FOR A MAGLEV SYSTEM

Thalles Denner Ferreira Cabral[1 §], Fábio Roberto Chavarette[2]

[1]UNESP - Universidade Estadual Paulista
Department of Mechanical Engineering
Brazil Avenue, 56, 15385-000, Ilha Solteira, SP, BRAZIL

[2]UNESP – Universidade Estadual Paulista
Department of Mathematics
Brazil Avenue, 56, 15385-000, Ilha Solteira, SP, BRAZIL

Abstract: Several experimental maglev systems all around the world, mainly in Germany and Japan have demonstrated that this mode of transportation can profitably compete with air travel. However, a system such as the German maglev train (called Transrapid) is inherently unstable. This instability is because the electromagnetic suspension (EMS) uses attractive force to levitate the train. So, the electromagnets of the vehicle must be actively controlled to make safe operation. Herewith, from a simplified model for the German Transrapid experimental system, we propose two control designs and, then we compare them. The linear quadratic regulator (LQR) is used to design the linear controller and the state-dependent Riccati equation (SDRE) is used to design the nonlinear controller. The simulation shows that the SDRE controller allows the maglev train to operate with much larger disturbances in the air gap than the LQR controller does.

AMS Subject Classification: 93C10
Key Words: computer simulation, dynamics systems, mathematical model, maglev system, optimal control

Received: January 19, 2015

§Correspondence author

1. Introduction

Maglev trains (Magnetic levitation transport) are transport systems that can achieve high speeds with low friction compared to conventional wheel-rail trains. Other factors that become the very interesting maglev trains technology is that it can ease traffic congestion and helps reduce negative environmental impacts. Several engineers around the world, have developed projects related with the maglev trains technology, being that some these projects are in a relatively advanced stage. Several experimental maglev systems all around the world, mainly in Germany and Japan have demonstrated that this mode of transportation can profitably compete with air travel [1] and [2].

The German maglev train is the first system that operates completely non-contact with the guideway and without wheels. German scientists have designed a system called Transrapid which uses the technology of electromagnetic suspension (EMS) to levitate a train (see Fig. 1a). The Transrapid maglev train has a $31.5km$ test track in Germany, Emsland (TVE) and is commercially operated in Shanghai, China, since 2004 [3].

The levitation occurs through electromagnets that are strategically positioned on a series of C-shaped arms. Thus, these electromagnets exert a force of attraction in the ferromagnetic plates installed on the flange of a T-Beam [2]. This configuration allows the maglev train levitate and has lateral stability.

An electromagnetic suspension (EMS) system such as of the Transrapid maglev train is inherently unstable. Therefore, the electromagnets of the vehicle must be actively controlled to make safe operation [3] and [4]. So, from a simplified model for the German Transrapid experimental system, we propose two control designs and, then we compare them. The paper is organized as follows. In Section 2, we present two simplified models for the German Transrapid experimental system. In Section 3, we discuss some issues about dynamics of the electromagnetic suspension (EMS) system. In Section 4, we present two control designs and the results of computer simulations. In Section 5, the conclusions are presented.

2. The Maglev Model

Figure 1b shows the magnetic levitation system of the Transrapid maglev train, which is simplified as a single mass system on a rigid guideway. The primary suspension consists of electromagnets. Suspension systems are dominant in determining the basic dynamic and vibrational behavior of the maglev vehicle. A two-degree-of-freedom model considering coupling effects of primary and secondary suspensions was studied by [5]. Note that the model presented in this paper hasn't got a secondary suspension, however, we can use it to simulate the vehicle vertical dynamics [1], [5] and [6].

(a) Electromagnetic suspension. (b) Simplified model.

Figure 1: Magnetic levitation system of the Transrapid maglev train.

where, mg is the vehicle weight (including the electromagnets), s_M is the vertical gap between the guideway and the vehicle, S_0 is the vertical gap between the guideway and the equilibrium position of the vehicle, $L(s_M)$, R, i_M and u_M are the coil inductance, resistance, current and voltage, respectively.

The inductance $L(s_M)$ is a nonlinear function of vehicle position (s_M). According to [7] various approximations have been used to determine the inductance. Such as [6], [8] and [9] we shall neglect the leakage flux and eddy current effects, so that the inductance varies with the inverse of vehicle position as follows:

$$L(s_M) = \frac{c}{s_M} \qquad \text{wherein,} \qquad c = \frac{\mu_0 N^2 A}{2} \tag{1}$$

where, μ_0 is the inductance constant, A is the pole area and N is the number of coil turns.

2.1. Nonlinear Model Maglev

The nonlinear motion equations of the model shown in Fig. 1b are:

$$\begin{aligned} m\ddot{s}_M &= -\frac{c}{2s_M^2} i_M^2 + mg \\ \dot{i}_M &= \frac{i_M}{s_M}\dot{s}_M - \frac{Ri_M}{c} s_M + \frac{u_M}{c} s_M \end{aligned} \tag{2}$$

The nonlinearities of the system come from the nonlinear inductance due to the geometry of the magnet and the inverse square magnetic force law [1]. Details of the derivation of the model are discussed in [4] and [6].

2.2. Linear Model Maglev

For small deviations from steady-state as shown in Fig. 1b, we can write:

$$s_M = S_0 + \delta s,\ i_M = I_0 + \delta i,\ u_M = U_0 + \delta u,\ \dot{S}_0 = 0,\ \dot{I}_0 = 0,\ U_0 = I_0 R \quad (3)$$

Equation 1:

The electromagnetic force of the magnetic levitation system (useful for next calculations) is found using the concept of co-energy [8]. To calculate it, we consider a linear relationship between the flux and the current, so that the force electromagnetic can be written as follows:

$$f(s_M, i) = -\frac{1}{2} i^2 \frac{dL(s_M)}{ds_M} \quad \Rightarrow \quad f(s_M, i) = \frac{c}{2}\left(\frac{i}{s_M}\right)^2 \quad (4)$$

The system has one equilibrium state at which the force electromagnetic exactly counterbalances the force due to gravity, i.e., $mg = f(S_0, I_0)$. So, substituting (3) into Eq. (2) and using (4), we have:

$$m\delta\ddot{s} = -\frac{c}{2}\left(\frac{I_0 + \delta i}{S_0 + \delta s}\right)^2 + \frac{c}{2}\left(\frac{I_0}{S_0}\right)^2$$

Equation 2:

Substituting (3) into Eq. (2), we have:

$$\delta\dot{i} = \frac{I_0 + \delta i}{S_0 + \delta s}\delta\dot{s} - \frac{R(I_0 + \delta i)(S_0 + \delta s)}{c} + \frac{(U_0 + \delta u)(S_0 + \delta s)}{c}$$

Finally, neglecting the terms of higher order and making some rearrangements, we obtain the linearized motion equations:

$$\begin{aligned} \delta\ddot{s} &= -\frac{cI_0\delta i}{mS_0^2} + \frac{cI_0^2\delta s}{mS_0^3} \\ \delta\dot{i} &= \frac{I_0}{S_0}\delta\dot{s} - \frac{RS_0}{c}\delta i + \frac{S_0}{c}\delta u \end{aligned} \quad (5)$$

3. Dynamics of Electromagnetic Suspension System

The nonlinear system (2) can be rewritten in state space as follows:

$$\begin{aligned}\dot{x}_1 &= \frac{x_3(u_M - Rx_1)}{c} + \frac{x_1x_2}{x_3}\\ \dot{x}_2 &= -\frac{cx_1^2}{2mx_3^2} + g\\ \dot{x}_3 &= x_2\end{aligned} \tag{6}$$

Similarly, the linearized system (5) can be rewritten in state space as follows:

$$\begin{aligned}\dot{x}_1 &= \frac{S_0(\delta u - Rx_1)}{c} + \frac{I_0}{S_0}x_2\\ \dot{x}_2 &= \frac{cI_0}{mS_0^2}\left(\frac{I_0}{S_0}x_3 - x_1\right)\\ \dot{x}_3 &= x_2\end{aligned} \tag{7}$$

The state variables x_1, x_2 and x_3 represent coil current, vertical velocity of the vehicle, and vertical gap between the guideway and the vehicle, respectively, for both systems (6) and (7). Rearranging (1), we can calculate the constant c as follows: $c = L(s_M)s_M$, however, when the vehicle is in the equilibrium state, we have $s_M = S_0$ and $L_0 = L(S_0)$, therefore, $c = L_0S_0$.

As we've seen previously, the system has one equilibrium state when the electromagnetic force exactly counterbalances the gravitational force and the vehicle hasn't got vertical velocity and acceleration. However, the equilibrium is a saddle node which is unstable in the sense of Lyapunov (see Fig. 2a). Details of the stability analysis are discussed in [1] and [4]. Table 1 shows the system parameters we used in our simulation.

$m[kg]$	$g[m/s^2]$	$S_0[m]$	$L_0[h]$	$R[\Omega]$	$u_M[v]$	$I_0[A]$	$\delta u[v]$
10000	9.8	0.01	0.1	1	140	u_M/R	$u_M - RI_0$

Table 1: Model parameters.

Figure 2 shows the phase portrait and a trajectory of the system (6) and (7) in the $x_2 - x_3$ projection.

Figure 2a shows the phase portrait of the linearized model (7) around equilibrium point, which is topologically orbitally equivalent to nonlinear model (6). However, in regions far from the equilibrium point, the linearized model doesn't

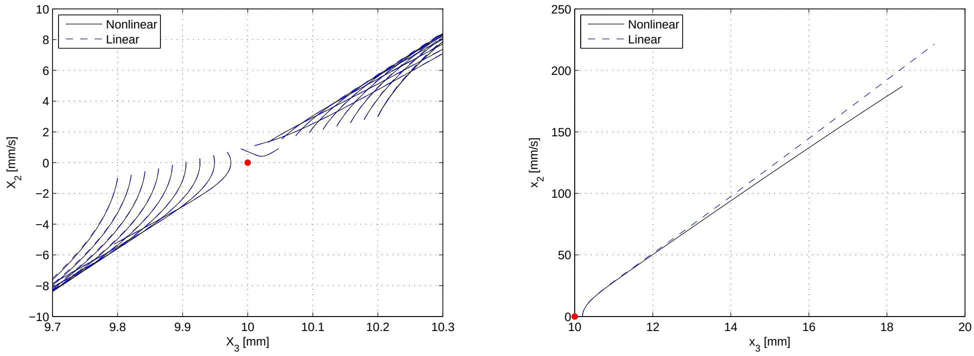

(a) Phase portrait. (b) Trajectory of the system.

Figure 2: Simulation computer system (6) and (7).

give good approximation the nonlinear model (see Fig. 2b). Therefore, linear controllers tend to saturate at the beginning of large initial displacements of the system equilibrium point [1].

4. Optimal Control Design

The control objective is to stabilize the maglev vehicle traveling above a guideway and, to maintain a constant distance between the vehicle and the guideway. The control parameter is the coil input voltage.

4.1. Control Design via Linear Quadratic Regulator

The LQR approach for obtaining an optimal solution of the control problem has the following procedure:

1. Represent the model in state-space form, and rewrite it as follows:

$$\begin{aligned} \dot{x} &= Ax + Bu \\ y &= Cx \end{aligned} \tag{8}$$

   where, $A \in \Re^{nxn}$ is the dynamic matrix, $B \in \Re^{nxm}$ is the input matrix, $C \in \Re^{sxn}$ is the output matrix, $x \in \Re^{n}$ is the state vector, $u \in \Re^{m}$ is the control law, $y \in \Re^{s}$ is the output vector.

2. Define the initial conditions $x(0) = x_0$, and choose the coefficients of positive definite weighting matrices Q and R, which determine the relative importance of state $x(t)$ and control effort $u(t)$, respectively.

3. Solve the Riccati equation given by:

$$A^T P + PA - PBR^{-1}B^T P + Q = 0 \tag{9}$$

4. Construct the linear feedback control via:

$$u = -R^{-1}B^T Px \tag{10}$$

The control law (10) is calculated so that the performance index given by, $J = \int_{t_0}^{\infty} (x^T Qx + u^T Ru)dt$ is minimized.

The technique LQR requires that the linear system is controllable. Details about the technique LQR can be found in [10] and [11].

Applying the above procedure in the linearized system (7), we obtain:

$$\dot{x} = \begin{bmatrix} -\frac{RS_0}{c} & \frac{I_0}{S_0} & 0 \\ -\frac{cI_0}{mS_0^2} & 0 & \frac{cI_0^2}{mS_0^3} \\ 0 & 1 & 0 \end{bmatrix} \begin{bmatrix} x_1 \\ x_2 \\ x_3 \end{bmatrix} + \begin{bmatrix} \frac{S_0}{c} \\ 0 \\ 0 \end{bmatrix} u \tag{11}$$

where, $u = \delta u$.

The system output and the coefficients chosen for the matrix Q and R are:

$$y = \begin{bmatrix} 1 & 0 & 0 \\ 0 & 1 & 0 \\ 0 & 0 & 1 \end{bmatrix} \begin{bmatrix} x_1 \\ x_2 \\ x_3 \end{bmatrix} \quad Q = \begin{bmatrix} 1 & 0 & 0 \\ 0 & 1 & 0 \\ 0 & 0 & 3.1\text{x}10^{12} \end{bmatrix} \quad R = \begin{bmatrix} 1 \end{bmatrix} \tag{12}$$

4.2. Control Design via State-Dependent Riccati Equation

The SDRE nonlinear regulator has the same structure of the linear quadratic regulator (LQR), except that all the matrices are state-dependent. The SDRE approach for obtaining a suboptimal solution of the control problem has the following procedure [12] and [13]:

1. Represent the model in state-space form. Use direct parametrization to bring the nonlinear dynamics $\dot{x} = f(x) + g(x)$ to the state-dependent coefficient (SDC) form, as follows:

$$\begin{aligned} \dot{x} &= A(x)x + B(x)u \\ y &= C(x)x \end{aligned} \tag{13}$$

where, $f(x) = A(x)x$ and $g(x) = B(x)$, $A(x) \in \Re^{nxn}$ is the dynamic matrix, $B(x) \in \Re^{nxm}$ is the input matrix, $C(x) \in \Re^{sxn}$ is the output matrix, $x \in \Re^n$ is the state vector $u \in \Re^m$ is the control law, $y \in \Re^s$ is the output vector.

2. Define the initial conditions $x(0) = x_0$, and choose the coefficients of positive definite weighting matrices $Q(x)$ and $R(x)$, which determine the relative importance of state $x(t)$ and control effort $u(t)$, respectively.

3. Solve the state-dependent Riccati equation given by:

$$A^T(x)P(x) + P(x)A(x) - P(x)B(x)R^{-1}(x)B^T(x)P(x) + Q(x) = 0 \quad (14)$$

4. Construct the nonlinear feedback control via:

$$u = -R^{-1}(x)B^T(x)P(x)x \quad (15)$$

The control law (15) is calculated so that the performance index given by, $J = \frac{1}{2}\int_{t_0}^{\infty}[x^TQ(x)x + u^TR(x)u]dt$ is minimized.

In the multivariable case, there always exists an infinite number of SDC parameterizations. Therefore, the choice of the matrix $A(x)$ isn't unique [12].

The pair $\{A(x), B(x)\}$ is a controllable parametrization of the nonlinear system in a region Ω if $\{A(x), B(x)\}$ is pointwise controllable in the linear sense for all $x \in \Omega$. Therefore, the choice of $A(x)$ must be such that the state-dependent controllability matrix $[B(x) \quad A(x)B(x) \quad \ldots \quad A^{n-1}(x)B(x)]$ has full rank [13].

The SDRE technique has been used to control various systems, such as agroecosystems [14], non-ideal systems with chaotic behavior [15], etc. Details about the technique SDRE can be found in [12] and [13].

Applying the above procedure in the nonlinear system (6), we obtain:

$$\dot{x} = \begin{bmatrix} -\frac{x_2}{x_3} & \frac{2x_1}{x_3} & -\frac{Rx_1}{c} \\ -\frac{cx_1}{mx_3^2} & 0 & \frac{cx_1^2}{2mx_3^3} \\ 0 & 1 & 0 \end{bmatrix} \begin{bmatrix} x_1 \\ x_2 \\ x_3 \end{bmatrix} + \begin{bmatrix} 0 \\ g \\ 0 \end{bmatrix} + \begin{bmatrix} \frac{x_3}{c} \\ 0 \\ 0 \end{bmatrix} u \quad (16)$$

where, $u = u_M$.

Assuming $C(x)$, $Q(x)$ and $R(x)$ are constant matrices, we have:

$$y = \begin{bmatrix} 1 & 0 & 0 \\ 0 & 1 & 0 \\ 0 & 0 & 1 \end{bmatrix} \begin{bmatrix} x_1 \\ x_2 \\ x_3 \end{bmatrix} \quad Q = \begin{bmatrix} 1 & 0 & 0 \\ 0 & 1 & 0 \\ 0 & 0 & 1.0085\text{x}10^8 \end{bmatrix} \quad R = \begin{bmatrix} 1\text{x}10^{-1} \end{bmatrix} \quad (17)$$

4.3. Computer Simulations

Assume that u is produced by a buck converter capable of delivering any voltage $0 \leq u \leq 450[V]$, and that the power supply delivers 140 volts at the equilibrium position of the vehicle. With respect to the state variables, consider the following domain of discourse for the analysis: $\{(x_1, x_2, x_3) \in \Re \mid 0 \leq x_1 \leq 300[A],\ -0.2 \leq x_2 \leq 0.2[m/s],\ 0 < x_3 \leq 0.02[m]\}$.

We emphasize that the control designs are in standard form. Therefore, we haven't considered constraints on the state variables $x(t)$ and control signal $u(t)$. Obviously, constraints such as the control signal saturation can be implemented, so, the results below may be different.

The responses of the controlled system (11) and (16) considering two different initial conditions are shown in Figs. 3, 4 and 5.

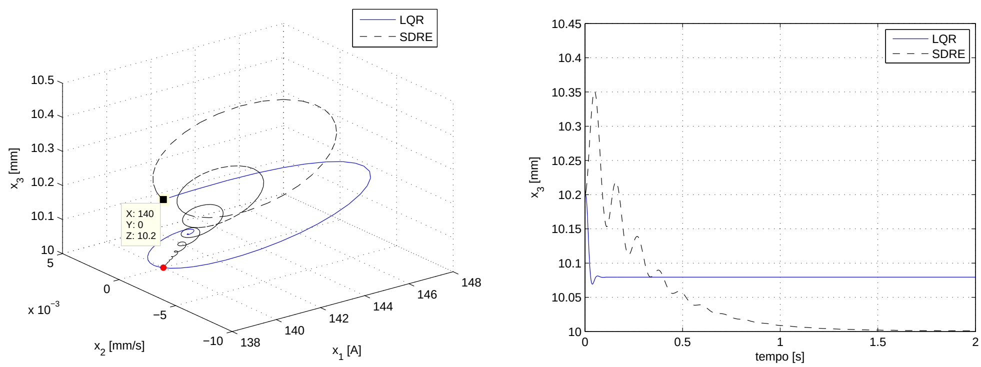

(a) Trajectory of the controlled system. (b) Time history of the vertical gap.

Figure 3: Response of the controlled system for $x(0) = (140, 0, 0.0102)$.

Table 2 shows some transient-response characteristics.

$x(0)$	Control	$x_{1max}[A]$	$x_{2max}[mm/s]$	$x_{3max}[mm]$	$u_{max}[V]$	$te[s]$
(140,0,0.0102)	*LQR*	147.87	-6.60	10.20	427.96	0.1
-	*SDRE*	147.01	-5.05	10.35	157.62	1.5
(140,0,0.015)	*LQR*	431.17*	-249.79*	15.00	10699*	0.1
-	*SDRE*	281.16	-80.73	16.64	448.39	1.5

Table 2: Some transient-response characteristics

In Tab. 2 the values with superscript (*) are outside of the domain of

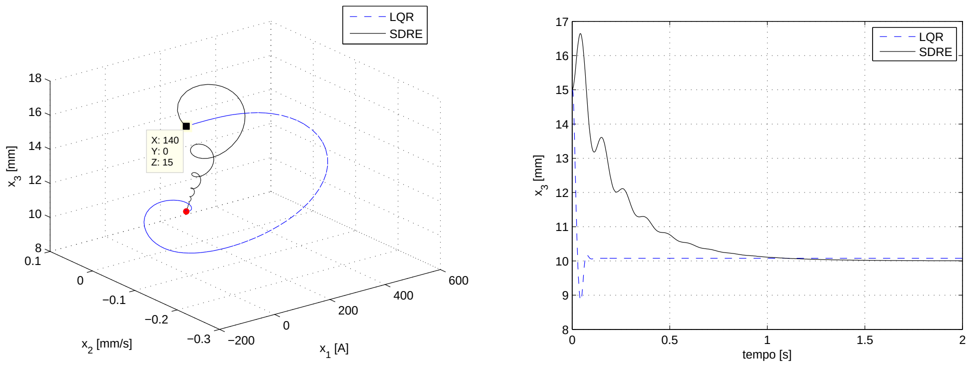

(a) Trajectory of the controlled system. (b) Time history of the vertical gap.

Figure 4: Response of the controlled system for $x(0) = (140, 0, 0.015)$.

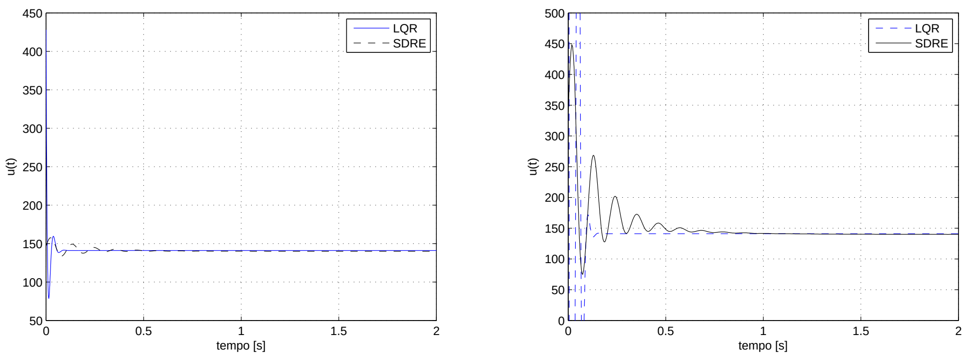

(a) $\mathsf{x}(0) = (140, 0, 0.0102)$. (b) $\mathsf{x}(0) = (140, 0, 0.015)$.

Figure 5: Control effort $u(t)$.

discourse.

5. Conclusion

The simulation results shows that both designed controllers are able to stabilize the vehicle traveling above a guideway. However, in the case of the LQR controller, the control signal amplitude is very high if we consider initial displacements $\delta s > 0.2mm$, so that the voltage required to bring the vehicle back to the equilibrium point is larger than the maximum voltage produced by buck converter, i.e., $u > 450V$. This is because the LQR controller design uses the linearized model (7) which doesn't give good approximation the non-linear model (6) in regions far from the equilibrium point (as seen in Section 3). On the other hand, the SDRE controller can bring the system back to the equilibrium with an initial displacement of up to $5mm$ from the equilibrium position. Furthermore, the control effort is less than in the LQR. With respect the settling time and maximum overshoot, the LQR controller is better than the SDRE controller. However, considering the domain of discourse of $x(t)$ and $u(t)$ we can said that the SDRE controller has better overall performance than the LQR controller. Moreover, the simulation shows that the SDRE nonlinear controller outperforms the linear controller LQR by a factor of 25 times with respect the maximum recoverable displacement.

Acknowledgment

The authors thanks Conselho Nacional de Pesquisas **CNPq** for financial supports (Proc. n° 132786/2013-3, Proc. n° 301769/2012-5).

References

[1] F. Zhao, R. Thornton, Automatic design of a maglev controller in state space, *Proceedings of the 31st Conference on Decision and Control*, **3** (1992), 2562-2567, **doi:** 10.1109/CDC.1992.371062.

[2] E. G. David, *O Futuro das Estradas de Ferro no Brasil*, Portifolium, Brasil (2009).

[3] H.-W. Lee, K.-C. Kim, J. Lee, Review of maglev train technologies, *IEEE Transactions on Magnetics*, **42**, No. 7 (2006), 1917-1925, **doi:** 10.1109/TMAG.2006.875842.

[4] T. D. F. Cabral, F. R. Chavarette, Anlise de estabilidade e projeto de controle pelo mtodo SDRE para um sistema maglev simplificado, *Anais do Congresso Nacional de Matemtica Aplicada a Indstria*, (2014).

[5] Y. Cai, S. S. Chen, Control of maglev suspension systems, *Journal of Vibration and Control*, **2**, No. 3 (1996), 349-368, **doi:** 10.1177/107754639600200305.

[6] G. Shu, R. Meisinger, State estimation and simulation of the magnetic levitation system of a high-speed maglev train, *International Conference on Electronic & Mechanical Engineering and Information Technology*, **2** (2011), 944-947, **doi:** 10.1109/EMEIT.2011.6023250.

[7] I. Ahmad, M. A. Javaid, Nonlinear model and controller design for magnetic levitation system, *Proceedings of the 9th WSEAS International Conference on Signal Processing, Robotics and Automation* (2010), 324-328.

[8] T. T. Salim, V. M. Karsli, Control of single axis magnetic levitation system using fuzzy logic control, *International Journal of Advanced Computer Science and Applications*, **4**, No. 11 (2013), 83-88, **doi:** 10.14569/IJACSA.2013.041111.

[9] A. Suebsomran, Optimal control of electromagnetic suspension EMS system, *The Open Automation and Control System Journal*, **6** (2014), 1-8, **doi:** 10.2174/1874444301406010001.

[10] K. Ogata, *Designing Linear Control Systems with MATLAB*, Prentice Hall, United States (1993).

[11] R. C. Dorf, *Sistemas de Controle Modernos*, Livros Tcnicos e Cientficos, Brasil (2001).

[12] J. R. Cloutier, C. N. D' Souza, C. P. Mracek, Nonlinear regulation and nonlinear H_∞ control via the state-dependent Riccati equation technique, *Proceedings of the International Conference on Nonlinear Problems in Aviation and Aerospace* (1996), 117-142.

[13] C. P. Mracek, J. R. Cloutier, Control designs for the nonlinear benchmark problem via the state-dependent Riccati equation method, *International Journal of Robust and Nonlinear Control*, **8** (1998), 305-461, **doi:** 10.1002/(SICI)1099-1239(19980415/30)8:4/5<401::AID-RNC361>3.0.CO;2-U.

[14] A. Molter, M. Rafikov, Controle timo em agroecossistemas usando SDRE, *Tendncias em Matemtica Aplicada e Computacional*, **12**, No. 3 (2011), 221-232, **doi:** 10.5540/tema.2011.012.03.0221.

[15] F. R. Chavarette, Control design applied to a non-ideal structural system with behavior chaotic, *International Journal of Pure and Applied Mathematics*, **86**, No. 3 (2013), 487-500, **doi:** 10.12732/ijpam.v86i3.3.